Modeling of an Electroactive Polyimide Ultrasonic Wave Sensor for Aerospace Applications

W. C. Wilson[*], G. M. Atkinson[**], D. F. Perey[*], M. A. Scott[*], and K. K. Tedjojuwono[*]

[*]NASA Langley Research Center, Hampton, VA, USA, w.c.wilson@larc.nasa.gov
[**]Virginia Commonwealth University, Richmond, VA, USA, gmatkins@vcu.edu

ABSTRACT

We have developed a new, low cost polyimide Capacitive Micromachined Ultrasonic Transducer (CMUT). The device will be constructed using an electroactive polyimide membrane and the PolyMEMS fabrication process developed at Virginia Commonwealth University. We have modeled the device to determine the deflection for a known pressure differential and to determine the minimum, maximum, and nominal capacitance that the device will generate. We have modeled the modes of vibration of the device and have investigated the strain induced during operation. This paper presents the results of the electromechanical modeling of this new device.

Keywords: microelectromechanical systems, MEMS, electroactive polymer, capacitive micromachined ultrasonic transducer, CMUT

1 INTRODUCTION

Ultrasonic techniques are useful in the non-destructive evaluation of aerospace vehicles. Cracks in metals and impact damage in composite structures can be monitored using Lamb waves [1]. MEMS transducers have been developed to detect ultrasonic waves [2]. The Capacitive Micromachined Ultrasonic Transducer (CMUT) sensor concept based on electroactive piezoelectric polyimide is one of these devices (figure 1).

We have developed a new, low cost polyimide CMUT device constructed using a polyimide membrane [3]. Polyimide was chosen as the construction material because it is chemically and thermally stable: it has excellent dielectric properties; it is durable and low cost [4]; and, it is compatible with standard integrated circuit processing techniques. A device made from polyimide will have better acoustic phase matching than that of Piezoelectric Micromachined Ultrasonic Transducer (PMUT) [5] and promises a cheaper and faster fabrication process than that used in conventional CMUTs [6].

The fabrication technique utilizes the simple, low cost PolyMEMS fabrication process developed at Virginia Commonwealth University [7]. The properties of sensors fabricated with polyimides can be tailored to fit many applications by combining additives to the material. Strontium ferrite particles can be added to a polyimide to make magnetic actuators [8], or molecular chains can be added to make the polyimide electroactive [9]. Therefore, this technique opens the door for construction of new types of sensors and devices based on the ability to adapt the properties of polyimides.

The sensor that we have developed consists of a membrane, suspended at two ends, and three electrodes (Figure 1). The membrane is 75 µm wide and 1000 µm long. The bottom electrode (green) is located on the silicon substrate and the top electrode (blue) is located on the underside surface of the membrane (yellow). The gap between the bottom electrode and the top electrode is 1.3 µm, and the bottom electrode is 50 µm wide. To facilitate testing and characterization, a third electrode (grey) has been added on top of the device. During operation, ultrasonic waves are coupled into the membrane from the supports causing the membrane to deflect. Deflection of the membrane is measured by the change in capacitance between the bottom and top electrodes.

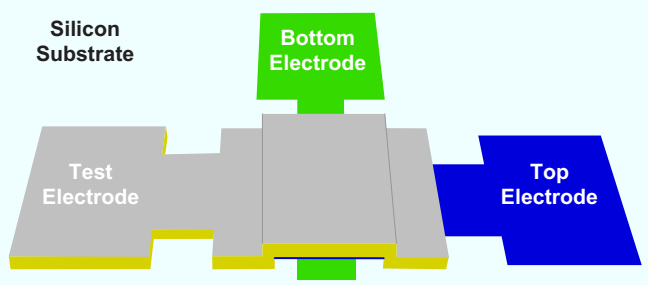

Figure 1: A concept for a polyimide Capacitive Micromachined Ultrasonic Transducer.

2 MODELING

The modeling for this device includes electrical, mechanical, and electromechanical modeling using Finite Element Analysis (FEA) methods. Variables that needed to be determined included the membrane displacement versus pressure, the capacitance versus membrane displacement, the mechanical modes of vibration, as well as the stresses and strains induced in our design. Harmonic analysis is required to yield the natural frequencies of major modes of vibration of the membrane. The layout and modeling was accomplished using CoventorWare® tools suite from Coventor, Inc. We have used the results of the simulations to design prototype devices that we will be fabricating at Virginia Commonwealth University.

2.1 Meshing

The first step in performing any kind of FEA involves the meshing of the device. For this device we employed Manhattan bricks that utilized a second order polynomial with parabolic elements that have 3 nodes along each edge for 27 nodes for each brick. Manhattan bricks fit well to the rectilinear shape of our device. Figure 2 shows the mesh used for the electromechanical simulations. The green blocks correspond to the bottom electrode.

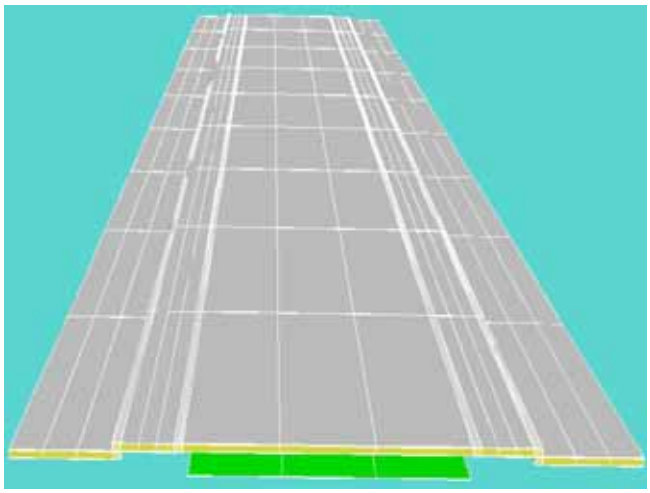

Figure 2: The membrane mesh using Manhattan bricks.

2.2 Membrane Deflection

We have modeled the device to determine the amount of deflection generated by a known pressure differential. This information is used to determine the minimum, maximum and nominal capacitance that the device will generate. A pressure of -0.1 MPa will deflect the membrane 834 nm upwards (Figure 3), while a 0.1 MPa pressure will deflect the membrane downwards 1019 nm.

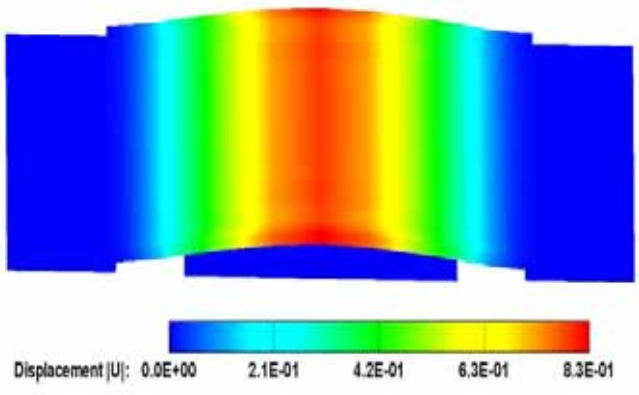

Figure 3: The deflection of the membrane for a -0.1 MPa pressure. The maximum upward displacement is 830 nm.

A parametric investigation of how the displacement and capacitance change as a function of pressure was performed. This data was used to generate the graph in Figure 4. The pressure is varied from -0.1 MPa to 0.1 MPa in 0.02 MPa increments. This causes the deflection to vary from 834 nm upwards to 1019 nm downwards. Correspondingly the capacitance varies from a minimum of 0.207 pF to a maximum of 1.577 pF, with the nominal capacitance of 0.341 pF when the membrane is not deflected.

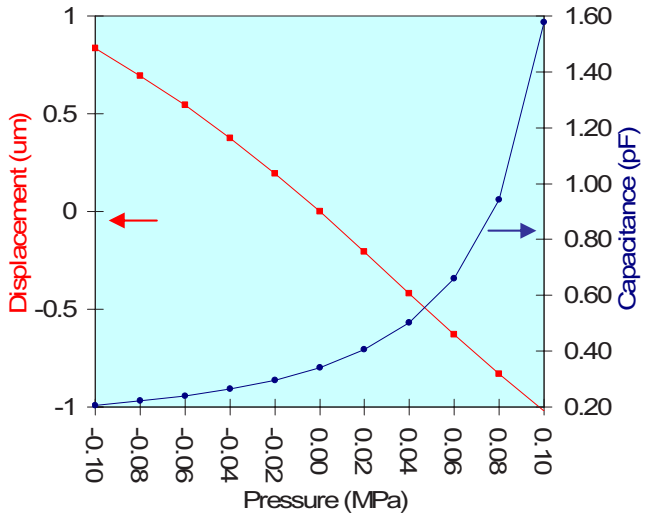

Figure 4: The effect of pressure changes from -0.1 MPa to 0.1 MPa on the displacement and capacitance of the membrane.

2.3 Modal Analysis

Modal analysis is a useful technique in the modeling of the dynamic behavior of a device. We have calculated the first four natural frequencies or modes of our membrane, the mode shapes and the displacement. The results are shown in Figures 5, 6, 7 and 8. Note that the maximum nodal displacements are normalized to ten and should only be used for relative comparisons. The modal analysis yields information on the natural frequencies and the generalized mass. Table 1 contains the frequencies and generalized mass for the first five modes.

Eigenmodes are used to calculate the harmonic response [10], and the equation for motion of the αth mode is given as follows:

$$\ddot{q}_\alpha + c_\alpha \dot{q}_\alpha + \omega_\alpha^2 q_\alpha = \frac{1}{m_\alpha} f_\alpha e^{i\Omega t}, \qquad (1)$$

where q_α is the αth mode amplitude, c_α is the αth mode damping coefficient, ω_α is the αth mode undamped frequency, m_α, is the αth mode's generalized mass, f_α is the αth mode amplitude forcing term, and Ω is the forcing frequency.

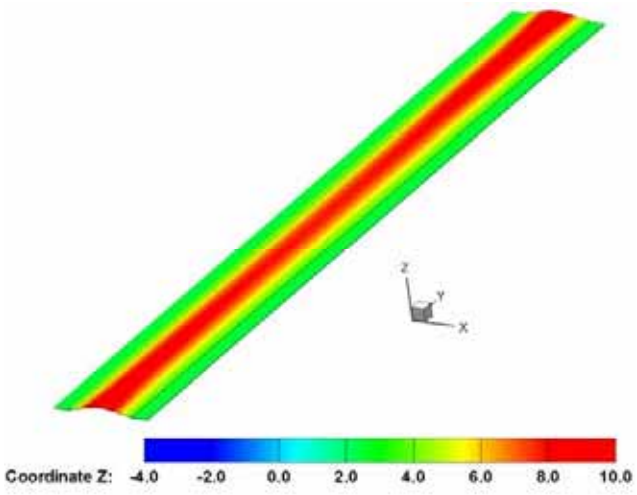

Figure 5: Membrane deflection for the first mode.

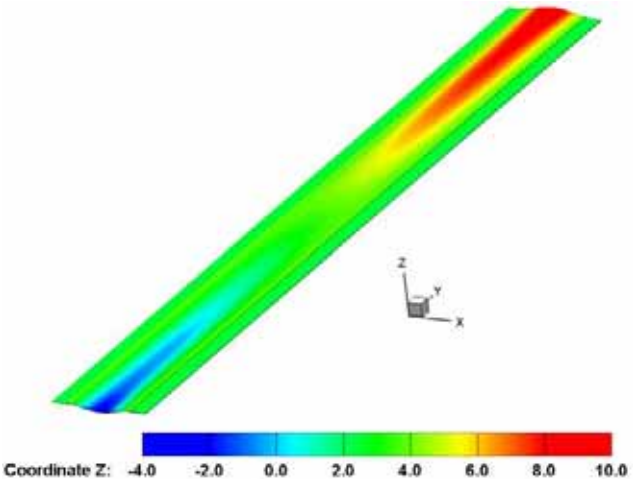

Figure 6: Membrane deflection for the second mode.

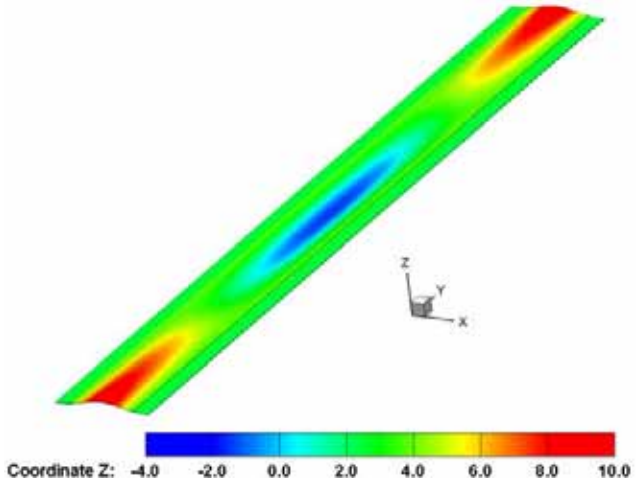

Figure 7: Membrane deflection for the third mode.

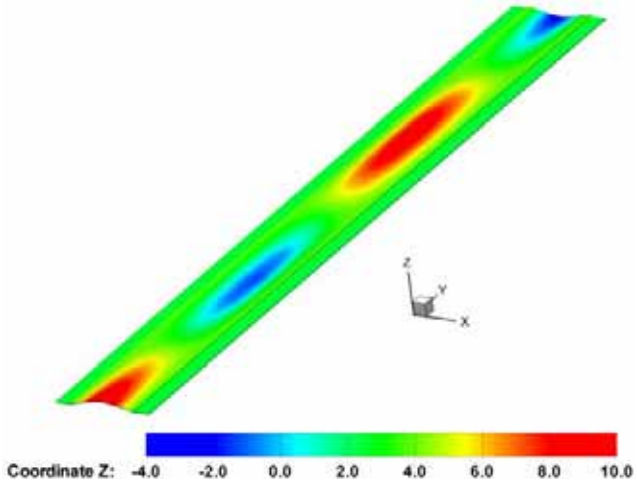

Figure 8: Membrane deflection for the fourth mode.

Mode	Frequency MHz	Generalized Mass 10^{-9}g
1	1.306402	29.14510
2	1.307949	16.75053
3	1.313996	19.63466
4	1.324101	19.16178
5	1.338645	18.18448

Table 1: Frequency and generalized mass for the first five modes.

2.4 Stress and Strain

A variety of stress results were obtained from our simulations. These included the three Principle Stresses, Mises, Tresca, and the Third Invariant Stress.

Figure 9 presents the Principle 1 stress results for the first mode 1. Three strain cases were also simulated S_{XX}, S_{YY}, and S_{ZZ}. Figure 10 shows the mode 1 strain results for S_{ZZ}. As one would expect the strain is mainly contained at the edges of the membrane.

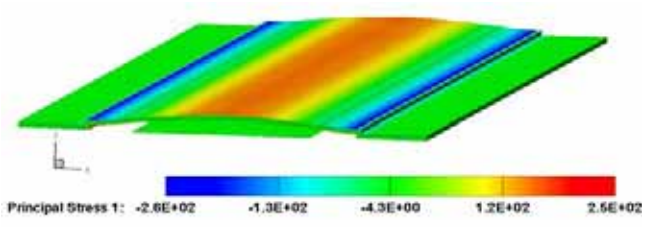

Figure 9: Principal Stress 1 for Mode 1.

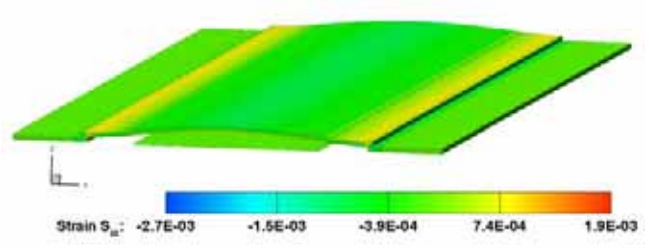

Figure 10: Strain S_{ZZ} results for Mode 1.

3 TEST STRUCTURES

In addition to our modeling efforts we have also fabricated test structures in the form of bridges to aid in the optimization of the fabrication process. The bridge structures should prove useful in the optimization of parameters such as the spinning speed, temperature, dwell time for the curing process, and polyimide viscosity necessary for a uniform film thickness. Also, the test structures gave us an opportunity to improve the process steps to get more uniform coverage of the polyimide. In figure 11 the long vertical line in the middle of the picture is the bottom electrode, the test electrode comes from the left side and extends over the bridge, and the top electrode is connected from the right hand side of the picture. The test devices included stiction bumps which can be seen sticking out from underneath the bridge structure in figure.

4 CONCLUSIONS

We have modeled a new, low cost polyimide Capacitive Micromachined Ultrasonic Transducer (CMUT). We have used the modeling to determine the displacement and capacitance changes for known pressure differentials. We have simulated the modes of vibration of the device, and have investigated the induced stresses and strains. We have fabricated test structures to determine process parameters that will be required for the fabrication of the device. We have used the results of the simulations to design prototype devices that will be fabricated at the Wright Virginia Microelectronics Center at Virginia Commonwealth University.

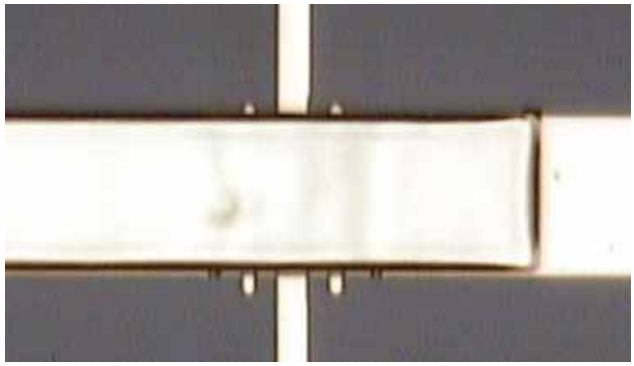

Figure 11: Photograph of a test structure. The stiction bumps appear as short vertical white lines below the bridge structure.

REFERENCES

[1] Lee, B C and Staszewski, W J, "Modeling of Lamb Waves for Damage Detection in Metallic Structures: Part I. Wave Propagation", Smart Mater. Struct., Vol. 12, No. 5, pp. 804-814, Oct. 2003.

[2] G. G. Yaralioglu, et al., "Lamb Wave Devices Using Capacitive Micromachined Ultrasonic Transducers", Appl. Phys. Lett., vol. 78, Jan 2001, pp. 111 – 113.

[3] W. C. Wilson, G. M. Atkinson, C. D. Armstrong, "An Electroactive Polyimide Lamb Wave Sensor Concept for Aerospace Applications", 2004 Solid State Sensor, Actuator and Microsystems, Hilton Head Island, SC, OP0048, June 6-10, 2004.

[4] B. Frazier, "Recent applications of polyimide to micromachining technology" Industrial Electronics, IEEE Transactions on, Vol. 42, Iss. 5, pp. 442 – 448, Oct. 1995.

[5] Igal Ladabaum, Xuecheng Jin, et al, "Surface Micromachined Capacitive Ultrasonic Transducers", IEEE Transactions on Ultrasonics, Ferroelectrics, and Frequency Control, vol. 45, no. 3, pp. 678-690, May 1998.

[6] M. H. Badi, G. G. Yaralioglu, et al, "Capacitive Micromachined Ultrasonic Lamb Wave Transducers Using Rectangular Membranes," IEEE Trans. on UFFC, Vol. 50, No. 9, pp. 1191-1203, Sept. 2003.

[7] G.M. Atkinson, et al, "Novel Piezoelectric Polyimide MEMS", Proc. of Conf. on Solid-State Sensors, Actuators and Microsystems, June 2003.

[8] L. K. Lagorce and M. G. Allen, "Magnetic and mechanical properties of micromachined strontium ferrite/polyimide composites", Journal of MEMS, vol. 6, no. 4, pp. 307-312, 1997.

[9] Cheol Park, Zoubeida Ounaies, Kristopher E. Wise, Joycelyn S. and Harrison, "In Situ Poling And Imidization Of Amorphous Piezoelectric Polyimides", NASA/CR-2002-211948 ICASE Report No. 2002-39, NASA Langley Research Center, pp. 20, Oct. 2002.

[10] Coventor Inc. Editors, CoventorWare Analyzer Tutorial Manual, Cary NC, Doc. Ver. 2004 Rev. A, pp. T4-20.